

Broadband saturable absorber for 10-fs pulse generation

R. Fluck, I. D. Jung, G. Zhang, F. X. Kärtner, and U. Keller

Ultrafast Laser Physics, Institute of Quantum Electronics, Swiss Federal Institute of Technology, ETH Hönggerberg-HPT, CH-8093 Zürich, Switzerland

Received November 13, 1995

We demonstrate the fabrication of a broadband saturable absorber with a silver bottom mirror. The reflectivity bandwidth of the absorber shows the potential for generating sub-10-fs pulses. With a Ti:sapphire laser we obtained self-starting Kerr-lens mode-locked pulses as short as 10 fs at the cavity stability limit and self-starting soliton mode-locked pulses of 16 fs over the full cavity stability regime. © 1996 Optical Society of America

Over the past few years considerable progress has been made in ultrashort-pulse generation with Ti:sapphire lasers. Pulses as short as 8 fs have been demonstrated directly from the laser oscillator.^{1,2} This rapid progress in pulse-width reduction is based on Kerr-lens mode locking³⁻⁶ (KLM) and considerable improvement in dispersion compensation.⁷ So far, to our knowledge no self-starting KLM lasers in the sub-50-fs regime have been demonstrated without an additional starting mechanism.⁸ It is important to note that in a 10-fs Ti:sapphire laser with a 100-MHz repetition rate, the peak power changes by 6 orders of magnitude when the laser switches from cw to pulsed operation. Therefore nonlinear effects that are still effective in the sub-10-fs regime are typically too small to initiate mode locking in the cw-operation regime. In contrast, if self-starting is optimized, either KLM tends to saturate in the ultrashort-pulse regime or the large self-phase modulation will cause the laser to become unstable. Therefore a reliable KLM-independent starting mechanism becomes indispensable for these lasers.

In this Letter we demonstrate that a broadband semiconductor saturable absorber can be designed to start a KLM laser in the 10-fs regime without limiting the pulse width (Fig. 1). In addition, we show that even without KLM, a similar absorber supports pulses as short as 16 fs in the soliton mode-locking regime^{9,10} over the full cavity stability regime.

In contrast, a pure KLM laser has to be operated at the stability boundary to enhance self-amplitude modulation sufficiently to achieve a large saturable absorber action. Saturable absorption that is due to self-focusing and self-phase modulation are interrelated because they are both produced by the intensity-dependent refractive-index change. However, if we insert an additional saturable absorber element, i.e., a semiconductor saturable absorber in our case, the important parameters such as the saturable absorption and the self-phase modulation coefficients can be optimized independently. As we show below the absorber can be designed to self-start the laser reliably without overdriving the nonlinearities at steady-state mode locking.

Previously we demonstrated pulses as short as 19 fs,¹¹ using a high-finesse antiresonant Fabry-Perot saturable absorber^{12,13} (A-FPSA) to start KLM. Pulses as short as 34 fs (Refs. 11 and 14)

have been demonstrated with an antireflection- (AR-) coated thin saturable absorber mirror that started and stabilized soliton mode locking over the full range of the cavity stability regime. In both cases the main limitation for further pulse-width reduction was the bandwidth of the lower AlGaAs/AlAs Bragg mirror. The small refractive-index difference between AlGaAs and AlAs fundamentally limits the reflection bandwidth of a Bragg mirror.⁷ Therefore, as a solution to this problem, we developed a process in which silver is used as a bottom mirror. This was not a trivial extension, because the semiconductor saturable absorber cannot be grown directly upon a silver mirror by molecular beam epitaxy (MBE). For the fabrication of such a broadband saturable absorber we had to use postgrowth processing: After MBE growth the semiconductor device was metallized with a silver layer and bonded to the Si substrate to provide good heat sinking.¹⁵ Afterward, the GaAs substrate had to be removed with a selective GaAs etching technique.¹⁶ Figure 2 shows the saturable absorber designs obtained when the broadband silver bottom mirror is used instead of a Bragg mirror. Because this device was used inside a solid-state laser cavity, the critical issues in this approach were how to obtain low insertion loss, good heat sinking, a sufficiently high damage threshold, and homogeneous performance over an area of approximately 5 mm × 5 mm.

The following is a detailed description of the fabrication process. First, the device structure was grown

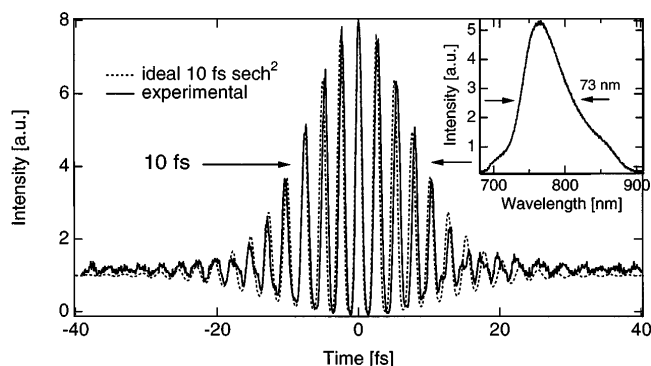


Fig. 1. Interferometric autocorrelation of a self-starting 10-fs KLM pulse by the use of a broadband low-finesse A-FPSA as a starting mechanism.

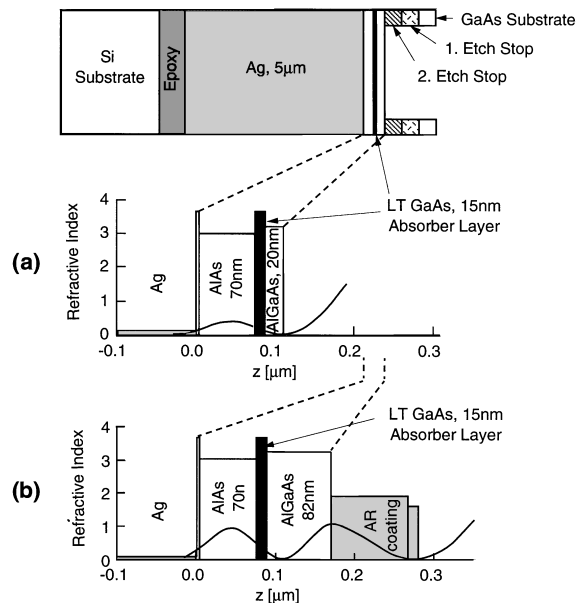


Fig. 2. Broadband saturable absorber design with a bottom silver mirror: (a) low-finesse A-FPSA, (b) thin AR-coated nonlinear reflector. The calculated standing-wave intensity distribution shows the location of the 15-nm-thick GaAs absorber layer with respect to the standing wave. The material layers before the etching process are shown partially removed. LT, low temperature.

upon a GaAs substrate by MBE. On the GaAs substrate, a 300-nm-thick $\text{Al}_x\text{Ga}_{1-x}\text{As}$ ($x = 0.65$) first etch-stop layer was grown for the selective GaAs etch, followed by a second etch-stop layer of 40-nm GaAs for the selective AlGaAs etch. This was followed by the top-side-down-grown structure of the low-finesse A-FPSA: On top of an $\text{Al}_x\text{Ga}_{1-x}\text{As}$ ($x = 0.65$) spacer layer is the low-temperature (400 °C) grown GaAs absorber layer, followed by another AlAs spacer layer. The device was capped by a 3-nm GaAs layer to prevent oxidation of the AlAs layer (Fig. 2).

Onto this MBE-grown structure, 5- μm silver was evaporated. Then the samples were cleaved in $\approx 5 \text{ mm} \times 5 \text{ mm}$ pieces and bonded upon a Si wafer with a two-component silver-filled epoxy to yield sufficiently good heat sinking. The samples were cured at 80 °C for at least 8 h with a 500-g weight on top. The GaAs was then lapped down to 100 μm and placed in a jet etcher with a $\text{NH}_4\text{OH}:\text{H}_2\text{O}_2$ (1:25) etch solution to selectively remove the remaining GaAs substrate and stop at the 300-nm AlGaAs etch-stop layer. The solution etches approximately 6 $\mu\text{m}/\text{min}$ at room temperature. The $\text{Al}_x\text{Ga}_{1-x}\text{As}$ etch-stop layer was then removed by a 1-min dip in HF. The 40-nm GaAs of the second etch-stop was etched in a less-concentrated $\text{NH}_4\text{OH}:\text{H}_2\text{O}_2$ (1:200) etch solution. To avoid nonuniform etching, the sample had to be agitated continuously. The edges of the sample and the exposed silver epoxy were protected by wax during the chemical etching. The wax was rinsed off with trichlorethylene.

We applied this process to two different saturable absorber structures. For the first case we chose a low-finesse A-FPSA with a thickness designed for antiresonance of the Fabry–Perot structure. This prevents ultrashort-pulse-width limitations owing to enhanced

wavelength-dependent reflectivity variations and enhanced group-velocity dispersion.¹⁷ The transparent spacer layers shift the absorber layer to a position in the standing-wave pattern (see Fig. 2) so that the wavelength-dependent absorption is balanced by the wavelength dependence introduced by the standing-wave intensity pattern. Figure 2(a) shows the thin low-finesse saturable absorber, which uses only a 15-nm-thick GaAs quantum-well absorber layer. The reflectivity is more than 94% at 800 nm, and the reflectivity curve shows only a slight wavelength dependence in the range of 700 to 1200 nm (Fig. 3). Around 870 nm one can see the smeared out absorption edge of GaAs. The calculated group delay of the thin low-finesse A-FPSA is less than 1 fs over a range of 200 nm.

Instead of designing the thickness of the low-finesse A-FPSA for antiresonance, one can design the thin saturable absorber for resonance and then cover it with an AR coating.¹⁴ An ideal AR coating removes all Fabry–Perot effects, resulting in a reflectivity curve similar to the Fresnel reflection of Ag/AlAs in our case. But a simple AR coating is correct only for one wavelength. For other wavelengths interference effects appear, leading to a stronger wavelength dependence of the reflectivity. Figure 2(b) shows the structure of the AR-coated thin saturable absorber with a 15-nm-thick GaAs quantum-well absorber layer sandwiched between 70-nm AlAs and 72-nm $\text{Al}_x\text{Ga}_{1-x}\text{As}$ ($x = 0.65$) spacer layers is also used. In this case the reflectivity is more than 93% over a wavelength range from 700 to 1200 nm. The reflectivity curve shows only a slight wavelength dependence owing to the AR coating. At 870 nm one can again see the absorption edge of GaAs. The calculated group delay of the thin saturable absorber is 5 fs at its center wavelength and increases to 9 fs within a 200-nm bandwidth.

We measured the impulse response and maximum modulation depth of both the low-finesse A-FPSA and the thin saturable absorber with 100-fs pulses in a standard degenerate pump–probe setup. For the thin low-finesse A-FPSA, we obtained a maximal modulation depth of 2% and a saturation fluence of 52 $\mu\text{J}/\text{cm}^2$, whereas for the thin saturable absorber with AR coating we obtained a modulation depth of 3.5% and a saturation fluence of 72 $\mu\text{J}/\text{cm}^2$. For the AR-coated thin

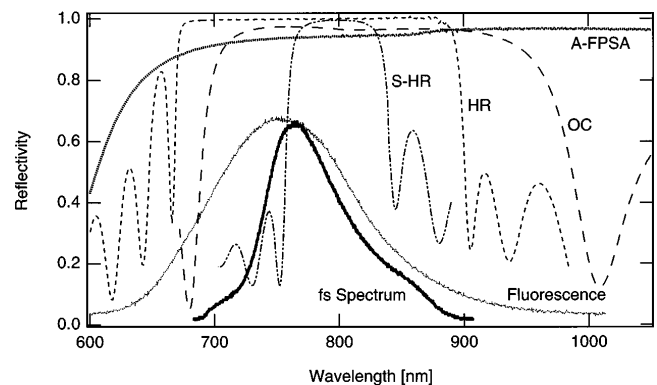


Fig. 3. Reflectivity of the thin low-finesse A-FPSA; 10-fs optical spectrum; fluorescence spectrum of Ti:sapphire; and output coupler (OC), Spectra-Physics high reflector (HR), and Bragg reflector (S-HR) curves.

saturable absorber, a higher modulation depth can be achieved, because more of the field couples into the absorber. The intensity on the semiconductor absorber can also be scaled by the focus of the laser beam. For both samples we measured a short time constant of approximately 200 fs owing to thermalization processes and a longer one (>10 ps) owing to interband recombination. The contribution of the short time constant is larger for the AR-coated sample.

In our experiments we used a standard dispersion-compensated delta cavity for the cw argon-ion-laser-pumped Ti:sapphire laser with two 10-cm focusing mirrors and a 2-mm-thick Ti:sapphire laser crystal (0.25% doping). A 10-cm focusing mirror reduced the beam radius to $36 \mu\text{m}$ on the saturable absorber. The 3% output coupler and the high-reflector mirrors are all from Spectra-Physics. For the 10-fs pulse we externally compensated the 3-mm-thick output coupler and the remaining third-order dispersion with chirped mirrors obtained from Szipöcs *et al.*⁷

Using the low-finesse A-FPSA as a mode-locking starting mechanism in combination with KLM close to the stability limit of the laser cavity, we obtained self-starting 10-fs pulses at a center wavelength of 765 nm (Figs. 1 and 3). The pulse-repetition rate was 86 MHz, and the average output power was 120 mW at a pump power of 4 W, which results in a pulse energy density of $1175 \mu\text{J}/\text{cm}^2$ on the thin saturable absorber. With the AR-coated thin saturable absorber we obtained self-starting 16-fs pulses at 830 nm over the full stability regime of the cavity. This is possible because of soliton mode locking⁹ stabilized by the slowly recovering absorber. The modulation depth of 3.5% of the AR-coated thin saturable absorber is strong enough to support the 16-fs pulses. However, the stabilization by the slow absorber was not so strong as the saturable action of KLM; therefore we had to move the center wavelength to 830 nm in order to reduce the residual third-order dispersion that destabilizes the solitonlike pulse.

The broadband absorber provides the same advantages with respect to the mode-locking mechanism as the absorbers on a Bragg mirror discussed in Ref. 11. But the new improved bandwidth of the absorber can support pulses even shorter than 10 fs. The bandwidth limitation in our experimental setup at long wavelengths is due to the group-velocity dispersion of the laser mirrors and the decrease of the gain of the Ti:sapphire crystal (Fig. 3). On the short-wavelength side, the reflectivity bandwidth and the group-velocity dispersion of the output coupler are more likely to limit the laser bandwidth than the losses of the low-finesse A-FPSA. Furthermore, higher-order dispersion most probably also limits the pulse width.¹⁸ The silver bottom mirror that we used provides a good heat sink for the semiconductor absorber, and therefore we observed no damage on the absorber at our intracavity intensities. However, the silver bottom

mirror introduces losses of approximately 2%. After the processing and additional AR coating the total nonsaturable losses of the nonlinear mirror increase to approximately 3–4%.

In conclusion, we have demonstrated a broadband thin low-finesse A-FPSA and an AR-coated thin saturable absorber, both with a silver bottom mirror, that were realized by the use of a selective GaAs etching technique. We discussed the advantages of an absorber with a silver bottom mirror versus a Bragg bottom mirror. The measured reflectivity curves and the calculated group delay of both discussed saturable absorbers have the potential bandwidth to produce sub-10-fs pulses. We generated 10-fs self-starting KLM pulses and 16-fs pulses by soliton mode locking, which does not require operation of the cavity close to the stability limit. This demonstrates the potential of semiconductor absorbers for ultrashort pulse generation.

This research was supported by the Swiss National Science Foundation. The authors thank H. Scherrer, L. R. Brovelli, K. Goossen, and H. Melchior and his group for helpful advice.

References

1. J. Zhou, G. Taft, C.-P. Huang, M. M. Murnane, H. C. Kapteyn, and I. P. Christov, *Opt. Lett.* **19**, 1149 (1994).
2. A. Stingl, M. Lenzner, Ch. Spielmann, F. Krausz, and R. Szipöcs, *Opt. Lett.* **20**, 602 (1995).
3. D. E. Spence, P. N. Kean, and W. Sibbett, *Opt. Lett.* **16**, 42 (1991).
4. U. Keller, G. W. 'tHooft, W. H. Knox, and J. E. Cunningham, *Opt. Lett.* **16**, 1022 (1991).
5. D. K. Negus, L. Spinelli, N. Goldblatt, and G. Feugnet, in *Advanced Solid-State Lasers*, G. Dubé, and L. Chase, eds. (Optical Society of America, Washington, D.C., 1991), p. 120.
6. F. Salin, J. Squier, and M. Piché, *Opt. Lett.* **16**, 1674 (1991).
7. R. Szipöcs, K. Ferencz, C. Spielmann, and F. Krausz, *Opt. Lett.* **19**, 201 (1994).
8. G. Cerullo, S. D. Silvestri, and V. Magni, *Opt. Lett.* **19**, 1040 (1994).
9. F. X. Kärtner and U. Keller, *Opt. Lett.* **20**, 16 (1995).
10. I. D. Jung, F. X. Kärtner, L. R. Brovelli, M. Kamp, and U. Keller, *Opt. Lett.* **20**, 1892 (1995).
11. I. D. Jung, L. R. Brovelli, M. Kamp, U. Keller, and M. Moser, *Opt. Lett.* **20**, 1559 (1995).
12. U. Keller, D. A. B. Miller, G. D. Boyd, T. H. Chiu, J. F. Ferguson, and M. T. Asom, *Opt. Lett.* **17**, 505 (1992).
13. U. Keller, *Appl. Phys. B* **58**, 347 (1994).
14. L. R. Brovelli, I. D. Jung, D. Kopf, M. Kamp, M. Moser, F. X. Kärtner, and U. Keller, *Electron. Lett.* **31**, 287 (1995).
15. H.-J. J. Yeh and J. S. Smith, *Appl. Phys. Lett.* **64**, 1466 (1994).
16. J. J. LePore, *J. Appl. Phys.* **51**, 6441 (1980).
17. L. R. Brovelli, U. Keller, and T. H. Chiu, *J. Opt. Soc. Am. B* **12**, 311 (1995).
18. I. P. Christov, H. C. Kapteyn, M. M. Murnane, C. P. Huang, and J. Zhou, *Opt. Lett.* **20**, 309 (1995).